

Reduced Length Design  
of 9.8 MHz APS/PAR Accelerator Cavity

Y. W. Kang

R. L. Kustom

J. F. Bridges

RF Group

Advanced Photon Source

Argonne National Laboratory

July 8, 1992

Revised September 15, 1992

## 1. Introduction

Designing low frequency tuned RF accelerating cavities for high power operation and with a cavity length  $\ell$  much less than a quarter wavelength is difficult without extra capacitive loading. One approach to shortening cavity length is to employ a folded coaxial structure as shown in Figure 1. In a reentrant coaxial cavity, one or more cylindrical conducting walls may be used to partially divide the space between the inner and the outer conductors to increase the electrical length of the cavity.

However, if the maximum radius of the cavity is specified, the characteristic impedance of the coaxial transmission line becomes lower as the number of folds increases. The reactance at the open end of a short circuited coaxial line is

$$Z_{in} = jZ_o \tan(\beta\ell) \quad (1)$$

where the characteristic impedance of the coaxial transmission line

$$Z_o = 60 \ln \frac{r_2}{r_1} \quad (2)$$

where  $r_2$  and  $r_1$  are the radii of the outer and inner conductors, respectively. With lower characteristic impedance of the transmission line,  $Z_o$ , Eq. (1) does not increase appreciably until the total line length  $\ell$  approaches  $\lambda/4$ .

If the electrical length and the diameter of a cavity are much smaller than a quarter wavelength, an extra capacitive loading is required somewhere in the cavity. As an example, take the folded cavity as shown in Figure 1. If the length  $\ell < 1.8 m$  and the diameter  $d < 1.2 m$  at  $10 MHz$ , then the cavity may need several hundreds of  $pF$  of extra capacitive loading at the junction of two transmission line sections to maintain a minimum of  $10 cm$  of separation between conductors in the coaxial structure for safe high power application. The capacitive loading may be realized by using one or more circular disks at the junction of the coaxial transmission line sections. A circular parallel plate capacitor with  $50 cm$  radius will have capacitance of about  $500 pF$  if the spacing between the plates is  $1.5 cm$ . However, this small spacing is not desirable for high voltage application.

By analogy of an equivalent  $L - C$  resonant circuit, greater capacitance is needed near the accelerating gap and greater inductance is needed near the short circuited end to reduce the cavity length. It will be shown later that in a folded structure, the coaxial section close to the gap needs lower  $Z_o$  to have greater capacitance and the coaxial section close to the short circuited end must have greater  $Z_o$  to have greater inductance. Eq. (2) suggests that using the outermost conductor for the low  $Z_o$  coaxial section and the innermost conductor for the high  $Z_o$  coaxial section is more efficient in getting a shorter cavity length for a specified cavity radius. A design of this cavity is shown in Figure 4.

The above cavities can be modeled as a circuit with transmission line sections and lumped elements. In the following, two configurations of the reduced length coaxial cavities are discussed; the folded cavity and the radial line loaded gap cavity are compared with design equations. The APS PAR 9.8MHz first harmonic cavity is designed in the two configurations and compared. Since capacitive loading in the reduced length cavities involves use of radial transmission line structure, the properties of radial transmission line are discussed. The results of URMELT simulations are presented and compared.

## II. Radial Transmission Line

For the dominant  $TEM$  to  $r$  mode of a parallel plate radial transmission line structure [1], the fields with inward and outward traveling waves are

$$\begin{aligned} E_z &= AH_o^{(1)}(kr) + BH_o^{(2)}(kr) \\ &= [J_o^2(kr) + N_o^2(kr)][Ae^{j\theta(kr)} + Be^{-j\theta(kr)}] \end{aligned} \quad (3a)$$

$$\begin{aligned} H_\phi &= \frac{j}{\eta}[AH_1^{(1)}(kr) + BH_1^{(2)}(kr)] \\ &= \frac{\sqrt{[J_o^2(kr) + N_o^2(kr)]}}{Z_o^w(kr)}[Ae^{j\psi(kr)} - Be^{-j\psi(kr)}] \end{aligned} \quad (3b)$$

where  $A$  and  $B$  are magnitudes of incident and reflected waves, and  $H^{(1)}$  and  $H^{(2)}$  are the Hankel functions of the first and second kind, respectively. The Hankel functions are

$$H_n^{(1)} = J_n + jN_n$$

$$H_n^{(2)} = J_n - jN_n$$

where  $J_n$  is the  $n$ -th order Bessel function of the first kind and  $N_n$  is the  $n$ -th order Bessel function of the second kind.  $Z_o(kr)$  is the characteristic wave impedance of a radial transmission line which is given as

$$Z_o^w(kr) = \eta \sqrt{\frac{J_o^2(kr) + N_o^2(kr)}{J_1^2(kr) + N_1^2(kr)}} \quad (4)$$

where  $\eta$  is the free space wave impedance.

The phase functions are

$$\theta(\nu) = \tan^{-1} \left[ \frac{N_o(\nu)}{J_o(\nu)} \right] \quad (5a)$$

$$\psi(\nu) = \tan^{-1} \left[ \frac{J_1(\nu)}{N_1(\nu)} \right]. \quad (5b)$$

The input impedance at a point  $r = r_i$  with a load impedance  $Z_L$  at  $r_L$  is

$$Z^b = Z_o(r_i) \frac{Z_L \cos\{\theta(kr_i) - \psi(kr_L)\} + jZ_o(r_L) \sin\{\theta(kr_i) - \theta(kr_L)\}}{Z_o(r_L) \cos\{\psi(kr_i) - \theta(kr_L)\} + jZ_L \sin\{\psi(kr_i) - \psi(kr_L)\}} \quad (6)$$

where the characteristic impedance is given as [2],

$$Z_o(r) = Z_o^w \frac{h}{2\pi r},$$

where  $h$  is the height of the radial transmission line.

The electric field or voltage reflection coefficient at  $r = r_i$  in the radial transmission line section is

$$\Gamma(r_i) = \Gamma(r_L) e^{2j\{\theta(kr_i) - \theta(kr_L)\}} \quad (7a)$$

and the magnetic field or current reflection coefficient at  $r = r_i$  in the radial transmission line section is

$$\Gamma(r_i) = \Gamma(r_L) e^{2j\{\psi(kr_i) - \psi(kr_L)\}} \quad (7b)$$

where

$$\Gamma(r_L) = \frac{Z_L - Z_o(r_L)}{Z_L + Z_o(r_L)}.$$

### III. Coaxial Cavity Designs

In the following section, design equations for the reduced length cavities are discussed with their equivalent circuits using transmission line sections and lumped elements. The voltage distributions in the cavities are also discussed.

#### A. Folded Coaxial Cavity

A coaxial cavity design employing a folded coaxial structure with lumped element loading is shown in Figure 1. The input impedance seen in the direction of the short circuited coaxial transmission line section at the position of the loading capacitance  $C_1$  is

$$Z^a = \frac{jZ_{o1}\tan\beta\ell_1}{1 - \omega C_1 Z_{o1}\tan\beta\ell_1}. \quad (8)$$

The input impedance seen in the other direction is

$$Z^b = jZ_{o2} \frac{Z_{o2}\omega C_2 \tan\beta\ell_2 - 1}{Z_{o2}\omega C_2 + \tan\beta\ell_2}. \quad (9)$$

At resonance  $Z^a = Z^{b*}$ , the loading capacitance  $C_1$  is solved as

$$C_1 = \frac{Z^{b*} - Z_{o1}\tan\beta\ell_1}{\omega Z_{o1} Z^{b*}\tan\beta\ell_1} \quad (10)$$

where \* denotes complex conjugate.

The voltage reflection coefficients at  $z = 0$  and  $z = \ell_2$  are

$$\Gamma(0) = \frac{Z^a - Z_{o2}}{Z^a + Z_{o2}} \quad (11a)$$

$$\Gamma(\ell_2) = \Gamma^*(0)e^{2j\beta\ell_2} \quad (11b)$$

where  $\Gamma^*(0)$  is used to satisfy the resonance condition. The voltages across capacitors  $C_1$  and  $C_2$  are

$$V(0) = V_m^+ \{1 + \Gamma(0)\} \quad (12a)$$

$$V(\ell_2) = V_m^+ e^{-j\beta\ell_2} \{1 + \Gamma(\ell_2)\} \quad (12b)$$

where  $V_m^+$  is the magnitude of the voltage wave traveling in  $+z$  direction. The voltage ratio is

$$\left| \frac{V_{C_1}}{V_{C_2}} \right| = \frac{|1 + \Gamma(0)|}{|1 + \Gamma(\ell_2)|}. \quad (13)$$

## B. Radial Transmission Line Loaded Gap Cavity

A coaxial cavity is shown in Figure 4. This design uses a parallel plate radial transmission line across the accelerating gap for the low  $Z_o$  structure. This configuration is useful in lowering the resonant frequency for a fixed cavity size, since the coaxial line section near the short circuit with  $Z_{o1}$  utilizes the beam pipe as the smaller radius of the center conductor, and the section closer to the gap with  $Z_{o3}$  utilizes the cavity outer wall as the outer conductor; lower  $Z_{o3}$  can be obtained by increasing the separation between the conductors.

The input impedance seen in the direction of the short circuited coaxial transmission line is, according to the equivalent circuit in Figure 4,

$$Z^a = Z_{o3} \frac{Z^A + jZ_{o3} \tan\beta\ell_3}{Z_{o3} + jZ^A \tan\beta\ell_3} \quad (14)$$

where  $Z^A$  is the input impedance at the junction  $J_2$  of the two transmission line sections connected in series,

$$Z^A = j(Z_{o1} \tan\beta\ell_1 + Z_{o2} \tan\beta\ell_2).$$

If the loading effect of the ceramic window is negligible, from Eq. (6) we have

$$Z^b = Z_o(r_i) \frac{\cos\{\theta(kr_i) - \psi(kr_L)\}}{j \sin\{\psi(kr_i) - \psi(kr_L)\}}. \quad (15)$$

At resonance  $Z^a = Z^{b*}$ , for a given resonant frequency, the length of the high impedance transmission line section  $\ell_2$  is found to be

$$\ell_2 = \frac{1}{\beta} \tan^{-1} \left( \frac{Z^{b*}(Z_3 - Z_1 \tan\beta\ell_1 \tan\beta\ell_3) - jZ_3(Z_1 \tan\beta\ell_1 + Z_3 \tan\beta\ell_3)}{Z_2(jZ_3 + Z^{b*} \tan\beta\ell_3)} \right). \quad (16)$$

Assuming an open circuit ( $\Gamma_{r_L} = 1.0$ ) at  $r = r_L$  which is the radius of the beam pipe, the voltage reflection coefficients at  $r = r_i$  is

$$\Gamma_{J1} = e^{2j\{\theta(kr_i) - \theta(kr_L)\}}. \quad (17a)$$

The voltages at  $r_L$  and at the junction of radial transmission line and outer coaxial structure of impedance  $Z_o3$ ,  $J1$ , are

$$\begin{aligned} V_{r_i} &= 2V_m^+ \\ V_{J1} &= V_m^+ e^{-j\{\theta(kr_i) - \theta(kr_L)\}} (1 + \Gamma_{J1}) \end{aligned} \quad (17b)$$

where  $V_m^+$  is the magnitude of the voltage wave traveling in the  $-r$  direction. At junctions  $J2$  and  $J1$ , the voltage reflection coefficients are

$$\Gamma'_{J2} = \frac{Z^A - Z_o3}{Z^A + Z_o3} \quad (18a)$$

and

$$\Gamma'_{J1} = \Gamma'_{J2} e^{2j\beta\ell_3}. \quad (18b)$$

The voltages at the junctions  $J2$  and  $J1$  are

$$V'_{J2} = V_m^{+'}(1 + \Gamma'_{J2}) \quad (19a)$$

$$V'_{J1} = V_m^{+'} e^{-j\beta\ell_3} (1 + \Gamma'_{J1}) \quad (19b)$$

where  $V_m^{+'}$  is the magnitude of the voltage wave traveling in the  $+z$  direction. Then

$$V_{J2} = \frac{V_{J1} V'_{J2}}{V'_{J1}}. \quad (20)$$

#### IV. Design Results and Discussions

Design equations are used to find the approximate dimensions and voltage distributions in the cavities for a specified fundamental mode frequency. Fine tuning of the cavity is made by using the computer simulation program URMELT.

For a folded coaxial cavity, the loading capacitance  $C_1$  with respect to the cavity length and the characteristic impedances  $Z_{o1}$  and  $Z_{o2}$  are shown in Figure 2 for the case of  $9.8MHz$  cavity. The cavity has a length  $\ell = 1.6m$ , a radius  $r_2 = 0.6m$ , and a  $13.0cm$  accelerating gap length. These results show that greater  $Z_{o1}$  for structure near gap and smaller  $Z_{o2}$  for structure near short circuit are required to lower the

resonant frequency of the cavity for a fixed cavity length. The voltage across  $C_1$  normalized with respect to the gap voltage across  $C_2$  is shown in Figure 3. The lower  $Z_{o2}$  requires smaller distance between the inner and the outer conductors, which is incompatible with high power operation. In order to increase the distance between the conductors, greater loading capacitance is required. In simulation using the URMELT code with the constraints  $\ell = 1.6m$ ,  $r_2 = 0.6m$ ,  $13.0cm$  of accelerating gap length, and  $10.0cm$  of conductor separation in the inner coaxial structure, more than  $500pF$  of extra capacitive loading is required. Table 1 shows the properties of the monopole and the dipole modes of the folded coaxial cavity obtained from the URMELT simulations.

Table 2 shows the length  $\ell_2$  versus the low  $Z_o$  coaxial line spacing  $d$  of the radial transmission line loaded gap cavity. This configuration is efficient in shortening cavity length and provides greater voltage handling capability. A design for  $9.8 MHz$  was used in an URMELT simulation for  $0.6m$  outer radius and  $1.6m$  total length. The accelerating gap length and the conductor spacing in the low impedance coaxial section have been chosen to be  $13cm$  and  $9cm$ , respectively. This gap length is considered to be sufficient for application of  $40KV$  in the APS PAR system. The URMELT input data is shown in Table 3. The monopole and dipole modes found from the URMELT simulation are listed in the Table 4.

Comparing simulation results of the folded and the gap loaded structures for the fundamental mode, the gap loaded design has higher  $R/Q$  by  $\sim 40\%$  and lower  $Q$  by  $\sim 15\%$  than the folded structure. Comparing the simulation results for the above two cavities, it can be seen that the higher order mode frequencies differ significantly and the monopole and dipole modes are ordered differently. In the cavity with the radial transmission line loaded gap, the second monopole mode has higher frequency with smaller  $R/Q$  and the third monopole mode has higher frequency with greater  $R/Q$  than the folded cavity.

## V. Acknowledgement

The authors would like to thank L. Emery for helpful comments, and having the URMELT code set up.

## References

- [1] Ramo, Whinery, and Van Duzer, "Fields and Waves in Communication Electronics," John Wiley and Sons, New York, 1965.
- [2] N. Marcuvitz, "Waveguide Handbook," IEE Electromagnetic Waves Series 21, 1986.

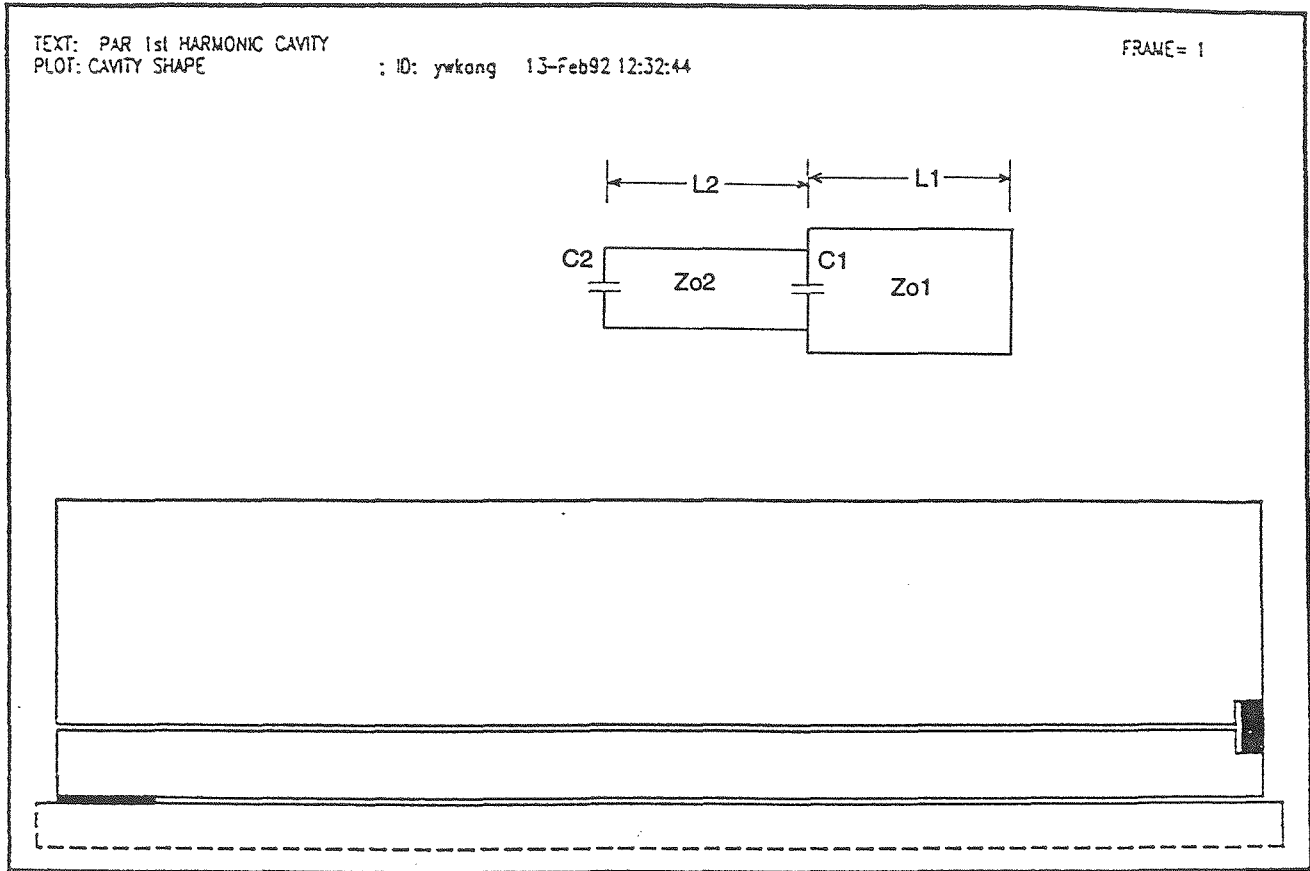


Figure 1. Cross-sectional view of the upper half of the folded coaxial cavity and equivalent circuit. Filled areas show dielectrics.

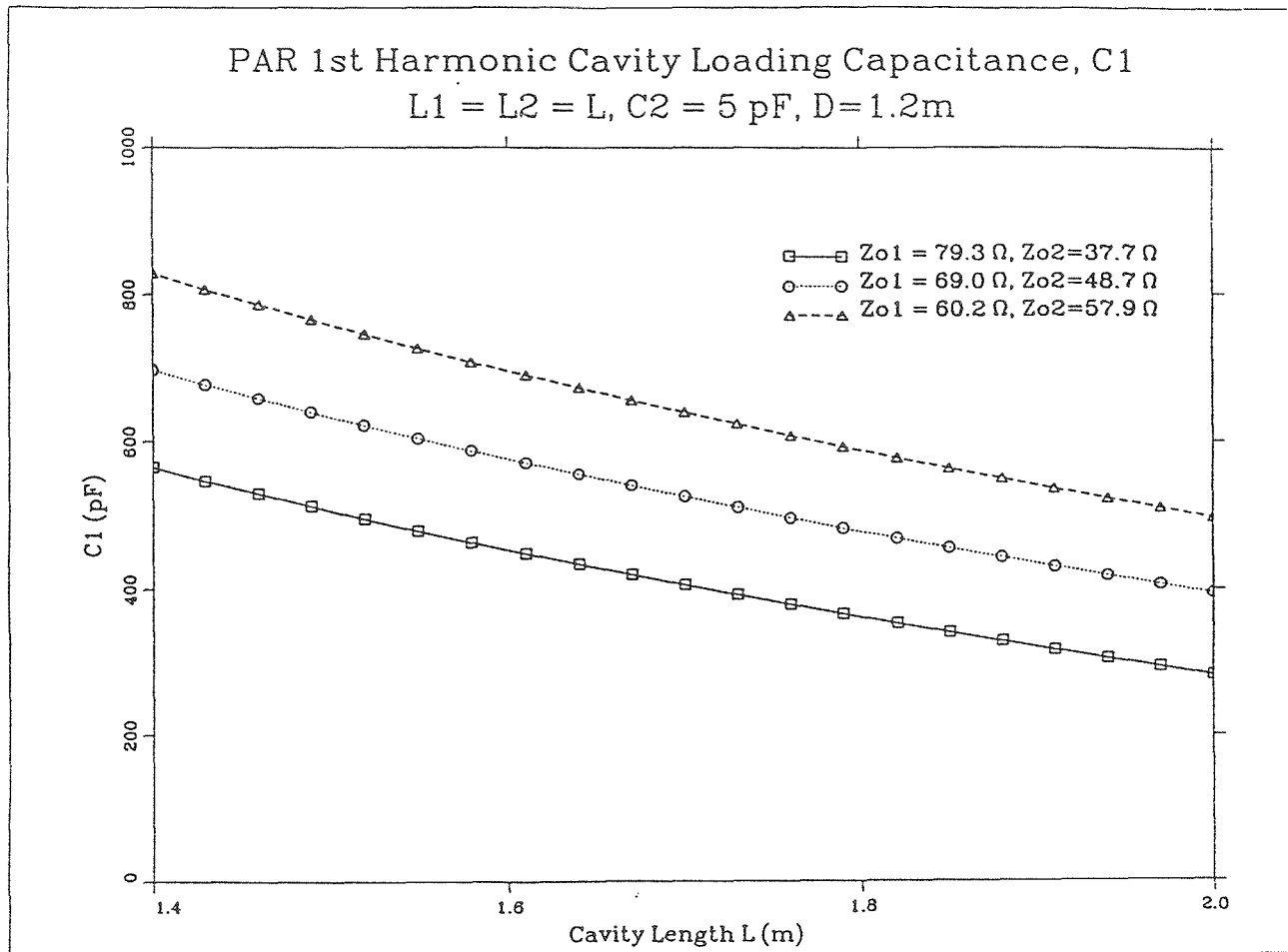


Figure 2. Loading capacitance  $C_1$  required at the junction of two transmission line coaxial sections vs. cavity length in the 9.8 MHz folded coaxial cavity.

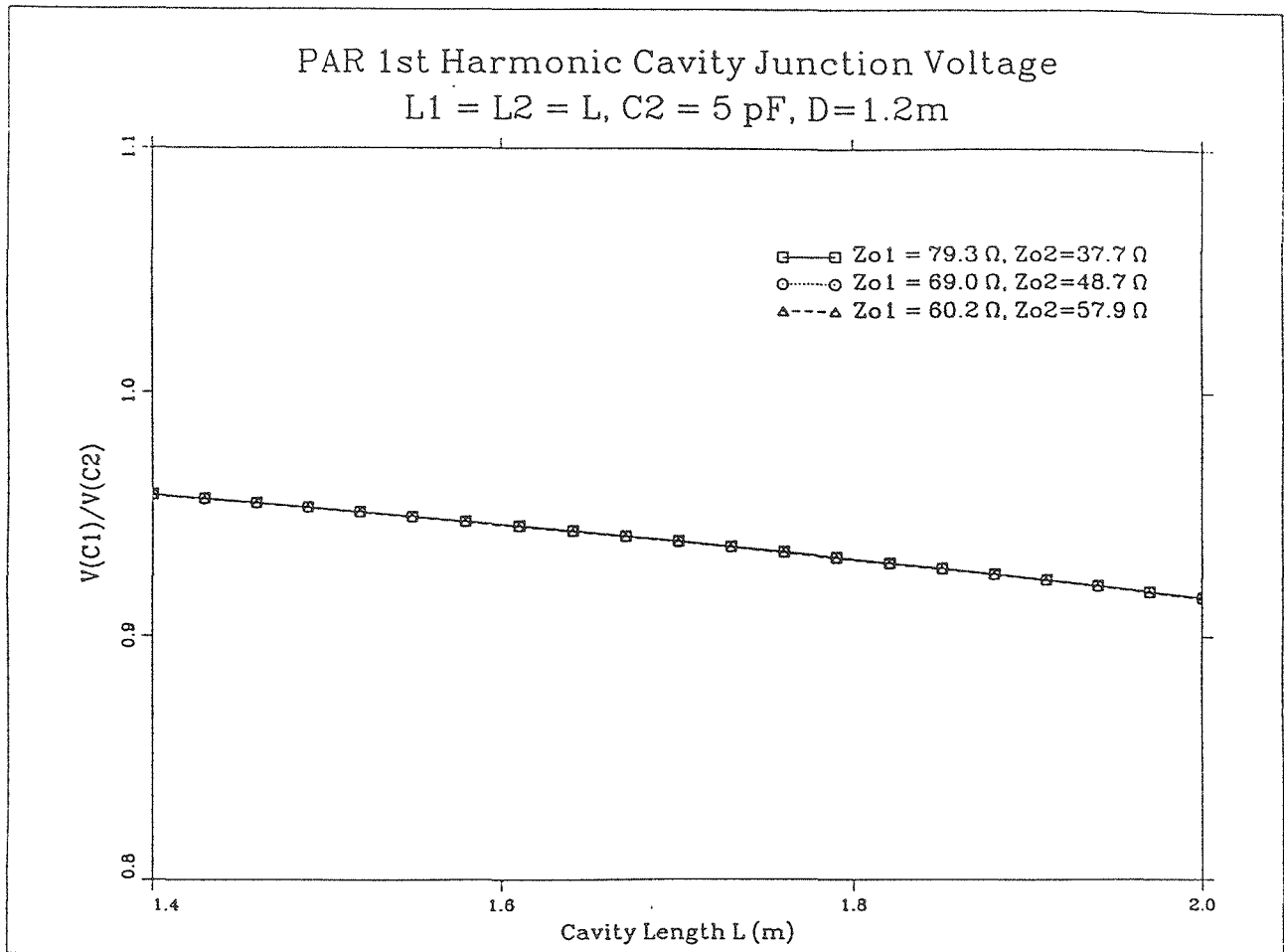


Figure 3. Voltage at the junction vs. cavity length in the 9.8 MHz folded coaxial cavity

Table 1. Computed modes for the 9.8 MHz folded coaxial cavity  
 TM<sub>0</sub>-monopole modes, TM<sub>1</sub>-dipole modes, EE-end plates  
 are electric wall. Voltage integrated at  $R_o = 0.0m$  off  
 axis for monopole modes and at  $R_o = 0.076m$  off axis for  
 dipole modes.

<i>MODE TYPE</i>	<i>FREQUENCY</i> (MHz)	$R/Q@R_o$ ( $\Omega$ )	$\frac{(R/Q)}{(K^*R_o)^{2M}}$ ( $\Omega$ )	$Q$	$R_s$ ( $M\Omega$ )
TM0-EE- 1	9.82	50.006		12689	0.635
TM0-EE- 2	49.88	107.786		9372	1.010
1-EE- 1	76.04	0.000	0.000	10040	0.000
TM0-EE- 3	97.24	0.201		34276	0.007
TM0-EE- 4	140.46	38.523		15537	0.599
1-EE- 2	157.28	0.000	0.000	58638	
TM0-EE- 5	192.41	0.102		47295	0.005
1-EE- 3	228.76	0.000	0.000	61723	
TM0-EE- 6	229.12	20.663		19096	0.395
TM0-EE- 7	285.11	1.174		40152	0.047
TM0-EE- 8	301.76	7.596		20838	0.158
1-EE- 4	311.19	0.000	0.000	56017	
TM0-EE- 9	339.01	5.773		26760	0.155
1-EE- 5	348.34	0.000	0.001	22296	
TM0-EE-10	361.91	2.141		36021	0.077
TM0-EE-11	370.14	1.629		35755	0.058
1-EE- 6	380.86	0.531	1.700	34455	0.018
TM0-EE-12	385.24	0.195		62691	0.012
1-EE- 7	385.64	0.856	2.676	40919	0.035
1-EE- 8	392.58	0.567	1.708	36631	0.021
TM0-EE-13	402.02	0.524		45193	0.024
1-EE- 9	404.69	0.215	0.610	66800	0.014
1-EE-10	413.29	2.901	7.891	35041	0.102
1-EE-11	423.94	0.417	1.077	47432	0.020
TM0-EE-14	426.02	6.464		28484	0.184
1-EE-12	426.69	0.001	0.002	55825	
1-EE-13	454.35	3.060	6.886	33734	0.103
1-EE-14	458.51	0.066	0.145	62425	0.004
1-EE-15	470.22	0.729	1.532	45742	0.033
TM0-EE-15	451.88	0.984		41699	0.041

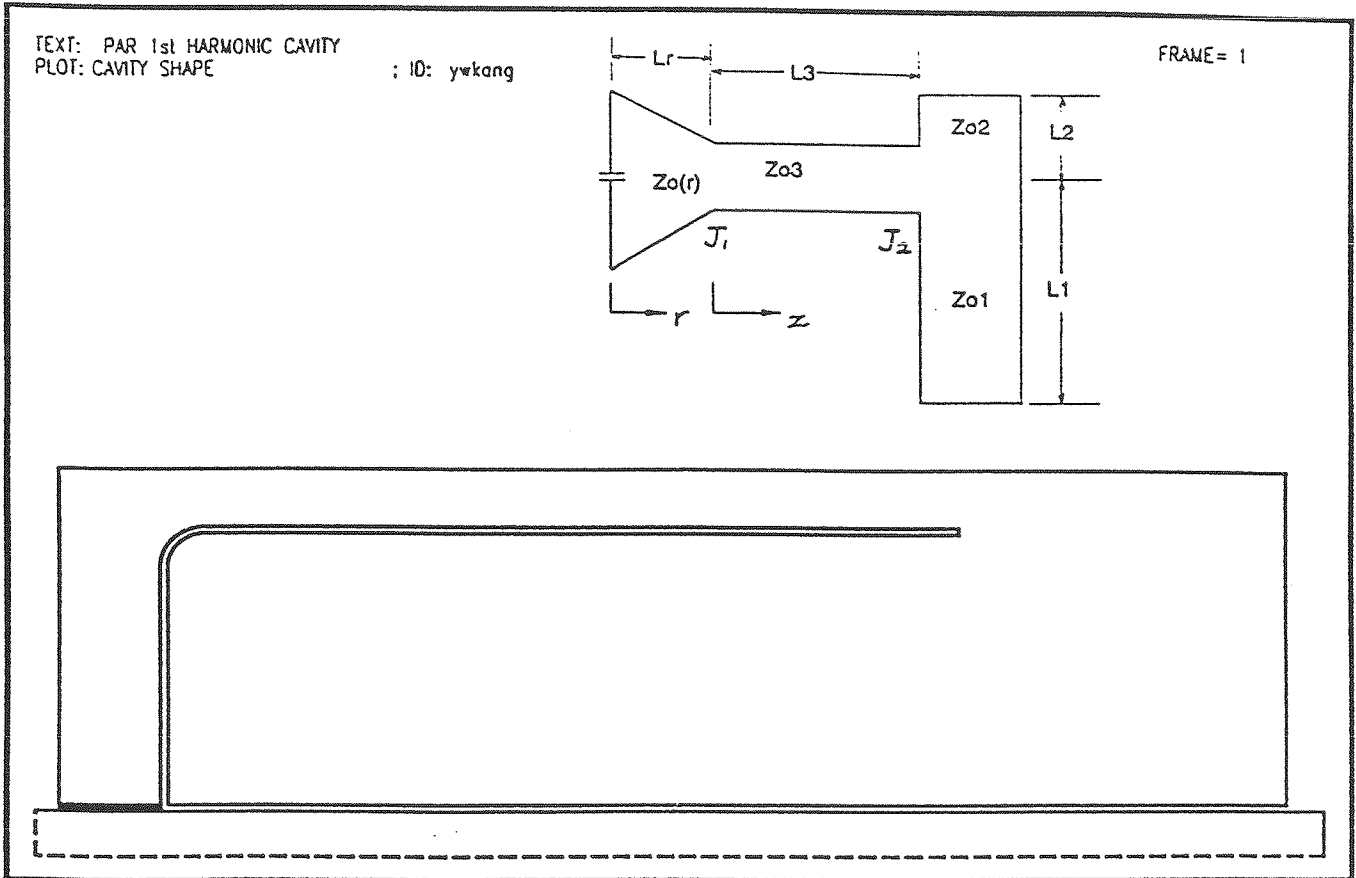


Figure 4. Radial transmission line loaded cavity and equivalent circuit

Table 2. Transmission line length  $\ell_2$  vs. conductor spacing of coaxial section with  $Z_o$  and voltages at  $J_1$  and  $J_2$  of radial line loaded coaxial cavity for  $9.8MHz$ .  $\ell_1 = 1.1m, r_o = 0.6m$ . Voltages are normalized to the gap voltage  $V_g$ .

$d(m)$	$\ell_2(m)$	$V_{J_1}/V_g$	$V_{J_2}/V_g$
0.100	0.583	0.968	0.935
0.095	0.493	0.968	0.935
0.090	0.402	0.967	0.934
0.085	0.312	0.967	0.934
0.080	0.222	0.967	0.934
0.075	0.125	0.966	0.934
0.070	0.043	0.966	0.934

Table 3. URMELT code input data for a radial line loaded cavity

```
$FILE LPLO=T ITEST=0 LXY=F $END
PAR 1st HARMONIC CAVITY
$BOUN $END
#MATDEF
3
(9.0,0.0) (1.0,0.0) 0
999
$MESH NPMAX=12000 MAT0=1 $END
#MATDIS
0 0
0.000 0.000
0.070 0.000
0.070 0.030
0.600 0.030
0.600 1.630
0.080 1.630
0.080 0.170
0.450 0.170
-1 -0.05
0.500 0.220
0.500 1.200
0.510 1.200
0.510 0.220
-1 0.06
0.450 0.160
0.070 0.160
0.070 1.680
0.000 1.680
0.000 0.000
8888 8888
3 3
0.070 0.030
0.080 0.030
0.080 0.160
0.070 0.160
0.070 0.030
8888 8888
9999 9999
$MODE MROT=0 NMODE=15 FUP=550 $END
$PLOT LCAVUS=F LMECI=F LMECU=F LMESH=F LFLE=F LFLH=F $END
$PRIN LER=F LEFI=F LEZ=F LHR=F LHFI=F LHZ=F $END
```

Table 4. Computed modes for the 9.8 MHz radial line loaded cavity  
 TM0-monopole modes, TM1-dipole modes, EE-end plates  
 are electric wall. Voltage integrated at  $R_o = 0.0m$  off  
 axis for monopole modes and at  $R_o = 0.076m$  off axis for  
 dipole modes.

<i>MODE TYPE</i>	<i>FREQUENCY</i>	$R/Q @ R_o$	$\frac{(R/Q)}{(K * R_o)^{2M}}$	$Q$	$R_s$
	(MHz)	( $\Omega$ )	( $\Omega$ )		(M $\Omega$ )
TM0-EE- 1	9.82	72.099		10581	0.763
1-EE- 1	95.27	0.235	12.051	16225	0.004
TM0-EE- 2	97.07	6.486		22692	0.147
TM0-EE- 3	112.59	18.509		17871	0.331
1-EE- 2	158.80	0.743	13.687	20027	0.015
TM0-EE- 4	188.90	30.781		22431	0.690
1-EE- 3	193.48	0.029	0.359	68873	0.002
TM0-EE- 5	204.95	0.264		43563	0.012
1-EE- 4	248.10	2.091	15.780	25594	0.054
1-EE- 5	260.76	0.019	0.129	78858	0.001
TM0-EE- 6	264.74	13.060		26939	0.312
TM0-EE- 7	300.87	2.378		43234	0.103
TM0-EE- 8	312.61	2.207		44475	0.098
1-EE- 6	314.68	2.939	13.789	33792	0.010
1-EE- 7	341.21	0.404	1.611	62147	0.025
TM0-EE- 9	351.79	0.012		48259	
1-EE- 8	353.97	0.748	2.772	59100	0.044
TM0-EE-10	366.11	13.643		31789	0.434
TM0-EE-11	395.21	0.888		49546	0.044
1-EE- 9	397.55	0.018	0.053	67793	0.001
1-EE-10	409.22	1.896	5.260	35667	0.068
TM0-EE-12	409.34	2.359		54637	0.129
TM0-EE-13	429.96	5.921		37694	0.223
1-EE-11	435.91	0.041	0.100	72831	0.003
1-EE-12	443.83	0.577	1.362	71480	0.041
TM0-EE-14	462.61	1.290		47689	0.062
1-EE-13	472.45	0.096	0.199	110536	0.011
1-EE-14	483.50	1.554	3.088	53130	0.083
TM0-EE-15	503.41	0.637		50661	0.032
1-EE-15	503.79	0.052	0.094	108312	0.006